ELSEVIER

Journal of Hepatology 42 (2005) 752–759

Journal of Hepatology

www.elsevier.com/locate/jhep

Hepatic phospholipids in alcoholic liver disease assessed by proton-decoupled ^{31}P magnetic resonance spectroscopy

Heinz-Peter Wilhelm Schlemmer[1], Tanja Sawatzki[2], Steffen Sammet[3], Ines Dornacher[2], Peter Bachert[3], Gerhard van Kaick[4], Rüdiger Waldherr[2], Helmut Karl Seitz[2,*]

[1]*Department of Diagnostic Radiology, University Hospital, Eberhard-Karls University, Tübingen, Germany*
[2]*Laboratory of Alcohol Research, Liver Disease and Nutrition, Department of Medicine, Salem Medical Center, Zeppelinstrasse 11-33, D-69121 Heidelberg, Germany*
[3]*Department of Medical Physics in Radiology, German Cancer Research Center (DKFZ), Heidelberg, Germany*
[4]*Department of Radiology, German Cancer Research Center (DKFZ), Heidelberg, Germany*

***Background/Aims*: Alteration of the phospholipid composition of hepatic biomembranes may be one mechanism of alcoholic liver disease (ALD). We applied proton-decoupled ^{31}P magnetic resonance spectroscopic imaging ({^{1}H}–^{31}P MRSI) to 40 patients with ALD and to 13 healthy controls to confirm that metabolic alterations in hepatic phospholipid intermediates could be detected non-invasively.**

***Methods*: All patients underwent liver biopsy. Specimens were scored in non-cirrhosis [fatty liver ($n=3$), alcoholic hepatitis ($n=2$), fibrosis ($n=4$), alcoholic hepatitis plus fibrosis ($n=16$)], and cirrhosis ($n=15$). {^{1}H}–^{31}P spectra were collected on a clinical 1.5-Tesla MR system and were evaluated by calculating signal intensity ratios of hepatic phosphomonoester (PME), phosphodiester (PDE), phosphoethanolamine (PE), phosphocholine (PC), glycerophosphorylethanolamine (GPE), and glycerophosphorylcholine (GPC) resonances.**

***Results*: The signal intensity ratio GPE/GPC was significantly elevated in cirrhotic (1.19 ± 0.22; $P=0.002$) and non-cirrhotic ALD patients (1.01 ± 0.13; $P=0.006$) compared to healthy controls (0.68 ± 0.04), while PE/PC and PME/PDE were significantly elevated in cirrhotic ALD patients compared to controls (1.68 ± 0.60 vs. 0.97 ± 0.31; $P=0.02$, and 0.38 ± 0.02 vs. 0.25 ± 0.01; $P=0.002$, respectively) and non-cirrhotic patients.**

***Conclusions*: The data support that {^{1}H}–^{31}P MRSI appears to distinguish cirrhotic from non-cirrhotic ALD patients and confirms changes in hepatic phospholipid metabolism observed in an animal model.**

***Keywords*: Phospholipid; Alcoholic liver disease; Cirrhotics; Phosphorus MR spectroscopy**

1. Introduction

Chronic alcohol consumption may lead to severe morphological and functional alterations of the hepatocyte including changes in the chemical composition and structure of biomembranes [1,2]. This membrane injury is predominantly caused by ethanol-induced changes in phospholipid metabolism [2,3]. It has been shown in rats and baboons, that chronic alcohol ingestion resulted in a decrease of hepatic polyenylphosphatidylcholine (PPC), a major constituent of biological membranes [4–6]. Various mechanisms contribute to the observed reduction of hepatic PPC, in particular, a lower production rate of phosphatidylcholine from phosphatidylethanolamine due to an acetaldehyde-mediated inhibition of phosphatidylethanolamine-*N*-methyltransferase (PEMT) [7,8]. Furthermore, chronic alcohol ingestion results in a reduced availability of the methyl groups that are necessary for phosphatidylcholine generation [9]. This disturbed hepatic methyl transfer is a result of various effects of alcohol

Received 11 June 2004; received in revised form 25 October 2004; accepted 1 December 2004; available online 11 March 2005

* Corresponding author. Tel.: +49 6221 483 200; fax: +49 6221 483 494.

E-mail address: helmut_karl.seitz@urz.uni-heidelberg.de (H.K. Seitz).

0168-8278/$30.00 © 2005 European Association for the Study of the Liver. Published by Elsevier B.V. All rights reserved.
doi:10.1016/j.jhep.2004.12.032

including folate, vitamin B_{12}, and vitamin B_6 deficiencies as well as decreased formation of *S*-adenosylmethionine (SAM), the active methylating compound [7,9–13].

Phosphorus-31 magnetic resonance spectroscopic imaging (^{31}P MRSI) has been applied in liver disease of various etiologies [14–23] as well as in alcoholics with [24,25] and without liver injury [26] to determine non-invasively relative concentrations of hepatic phosphorus-containing compounds. A ^{31}P MR spectrum of the human liver in vivo shows intense resonances of (a) phosphomonoesters (PME), containing information on the membrane-phospholipid precursors phosphocholine (PC) and phosphoethanolamine (PE), (b) phosphodiesters (PDE), containing information on the cell-membrane degradation products glycerophosphorylcholine (GPC) and glycerophosphorylethanolamine (GPE), (c) inorganic phosphate (P_i), and (d) adenosine 5′-triphosphate (ATP). In previous ^{31}P MR spectroscopy (MRS) liver studies, only the abnormalities of relative PME and PDE concentrations in patients with alcoholic liver disease (ALD) were measured [22,24–26] because with conventional ^{31}P MRS it is impossible to resolve the constituents of the PME and PDE resonances. The PME resonance is comprised of signals from PE and PC, and the PDE resonance is comprised of signals from GPE and GPC. Resolved resonances of PE, PC, GPE and GPC can be obtained by means of proton-decoupled ^{31}P MRSI ($\{^1H\}$–^{31}P MRSI) [27]. Proton decoupling is a double resonance technique that causes a collapse of scalar-coupled multiplets into singlets so that resonances become detectable. Thus, in the present study this method was used to determine whether ethanol-mediated changes in the hepatic membrane phospholipid compostition observed in rodents and baboons can also be detected in humans, and, if so, whether differences between various types of ALD can be seen.

2. Methods and materials

2.1. Patients

The study included 40 chronic alcoholics (29 males, 11 females; mean age: 49 years) with a daily alcohol intake of more than 100 g who were admitted to the Dept. of Medicine, Salem Medical Center Heidelberg for alcohol detoxification therapy or for therapy of complications of ALD, and 13 healthy volunteers (7 males, 6 females; mean age: 35 years) with an alcohol intake of less than 100 g per week. All patients underwent standardized serum analysis, ultrasound imaging, and liver biopsy as part of their initial clinical assessment. Patients with hepatitis B and C and autoimmune hepatitis were excluded from the study. Liver biopsy was performed under sonographic control from lateral (segment VII) using a standard biopsy needle with a diameter of 0.9 mm. The length of the biopsy was approximately between 1.5 and 2.0 cm. Biopsy area and the area of spectroscopic analysis were most frequently identical and in some cases rather close to each other. Biopsy specimens were scored in non-cirrhosis [fatty liver ($n=3$), alcoholic hepatitis ($n=2$), fibrosis ($n=4$), fibrosis plus hepatitis ($n=16$)] and cirrhosis ($n=15$). In addition, the percentage of hepatic fat was evaluated histologically. Patient and laboratory data are listed in Table 1. For statistical reasons we grouped the patients with steatosis, hepatitis, and fibrosis and referred to them as non-cirrhotics (NC) ($n=25$). Accordingly, we compared healthy controls (HC), NC, and cirrhotics (C).

The study was approved by the Ethical Committee of the University of Heidelberg and each person gave written consent.

2.2. Proton-decoupled ^{31}P MR spectroscopic imaging ($\{^1H\}$–^{31}P MRSI)

Patients were examined 4–20 days after their last alcohol consumption. $\{^1H\}$–^{31}P MRSI was performed using a clinical 1.5-Tesla MRI system (Magnetom Vision; Siemens, Erlangen, Germany), which was equipped with two radiofrequency systems enabling proton-decoupling during ^{31}P signal detection. A double-tuned (^{1}H, ^{31}P) planar surface coil with two concentric loops (14 cm diameter of ^{31}P-loop) was applied for spin excitation and signal detection. The surface coil was embedded in the table of the tomograph and patients were placed in right lateral position. Scout view images were obtained in three orthogonal directions for checking correct patient positioning. The ^{1}H-loop was used for MR imaging, adjusting the magnetic field homogeneity (shim), and decoupling. The ^{31}P-loop was used to acquire spectroscopic data.

Interactive shim was performed by monitoring the proton resonance of tissue water within the sensitive volume of the ^{1}H-loop. The linewidth at half height of the water resonance was in the order of 20–50 Hz.

Localized ^{31}P MR spectra were obtained with two-dimensional spectroscopic imaging (repetition time [TR] = 1100 ms; field-of-view [FOV] = 250 mm, slice thickness = 50 mm, 8×8 phase encoding steps, voxel size = 30×30×50 mm^3 = 45 ml). The number of excitations was 20 resulting in a total measurement time of 23.5 min for a single SI data set comprising 64 localized ^{31}P MR spectra. Additionally, a single prepulse was applied at ^{1}H frequency of tissue water to enhance the phosphorous signal intensity (nuclear Overhauser effect) [28–30]. Broadband proton-decoupling was achieved by a series of composite pulses irradiated at ^{1}H frequency during ^{31}P signal detection (WALTZ-8 with 128-ms length of pulse train) [31]. The equipment for double resonance (second radio frequency transmitter, double-tuned surface coil, pulse sequences) was purchased from Siemens and was certified by the manufacturer which also ensured that the specific absorption rate in decoupling experiments was always below the recommended limits.

The total examination lasted on average 60 min including positioning of the patient, acquisition of the images, shim, and data acquisition.

2.3. Spectroscopic data analysis

Spectroscopic data were processed using a commercial program (LUISE; Siemens) available at the Magnetom Vision scanner. To evaluate spectroscopic signal exclusively from the liver, the voxel grid was superimposed on MR scout images and then carefully shifted until one voxel was located adjacent to the center of the coil, and completely within the liver (Fig. 1). The correct positioning of the voxel entirely within the liver was verified by the weak phosphocreatine (PCr) signal in the MR spectrum, because PCr is absent in the liver parenchyma and originates from muscles in the abdominal wall only. Contamination from neighbouring voxels to the VOI is inherent to the applied SI technique particularly due to the relatively large voxel size.

Signal postprocessing included zero-filling to 2k data points, line-broadening (by multiplication with an exponential function), and Fourier transformation, followed by interactive phase and baseline correction. The resulting Fourier spectra were analyzed using the least-squares fit algorithm in LUISE and assuming a Lorentzian lineshape for each peak.

Signal intensities of PE (chemical shift $\delta = 7.1$ ppm), PC ($\delta = 6.5$ ppm), GPE ($\delta = 3.5$ ppm), GPC ($\delta = 2.9$ ppm), PCr ($\delta = 0$ ppm, endogenous chemical shift reference), anorganic phosphate (P_i, $\delta \cong 5$ ppm, depending on intracellular pH), and α-, β- and γ-ATP ($\delta = -7.6$, -16.0, -2.4 ppm, respectively) were obtained by integration of the fits of the resonances (Fig. 1). The sum of the intensities of PE and PC as well as of GPE and GPC were defined as signal intensity of PME and PDE, respectively.

2.4. Statistics

Statistical analysis of signal intensity ratios of the various resonances was performed by means of ANOVA (ANalysis Of VAriance) and unpaired

Table 1
Age, gender, histology, laboratory profile, and ascites in patients with alcoholic liver disease

Pat Nr.	Age (years)	Sex	Histology/(child) [% fat]	Bilirubin (mg/dl)	AP U/l	AST U/l	ALT U/l	GGT U/l	INR	Albumin (g/dl)	Ascites (+/−)
1	43	F	Steatosis [70]	1.84	95	56	39	40	1.05	4.22	(−)
2	45	M	Steatosis [60]	1.07	136	85	33	73	1.0	4.11	(−)
3	57	F	Steatosis [50]	0.69	109	37	18	339	1.0	n.e.	(−)
4	41	F	Hepatitis [60]	0.75	131	90	65	224	1.0	4.32	(−)
5	41	M	Hepatitis [50]	0.30	104	19	26	55	1.0	5.45	(−)
6	44	M	Fibrosis [30]	1	83	45	36	152	1.0	4.22	(−)
7	55	F	Fibrosis [50]	0.51	86	24	18	33	1.0	n.e.	(−)
8	45	M	Fibrosis [30]	0.48	66	12	10	38	1.0	4.58	(−)
9	31	M	Fibrosis [60]	0.41	158	67	56	374	1.0	4.51	(−)
10	44	M	Fibrosis + hepatitis [10]	1.63	86	25	22	15	1.0	4.56	(−)
11	53	M	Fibrosis + hepatitis [60]	1.43	67	24	25	44	1.0	3.68	(−)
12	62	M	Fibrosis + hepatitis [80]	14.27	306	80	36	245	1.0	3.9	(−)
13	38	M	Fibrosis + hepatitis [70]	1.03	89	89	104	160	1.0	5.12	(−)
14	42	M	Fibrosis + hepatitis [50]	0.56	86	32	25	291	1.05	3.61	(−)
15	63	M	Fibrosis + hepatitis [60]	1.1	83	25	38	90	1.10	4.55	(−)
16	49	F	Fibrosis + hepatitis [80]	1.2	154	57	40	197	1.0	4.66	(−)
17	37	M	Fibrosis + hepatitis [75]	0.41	92	33	47	166	1.0	5.12	(−)
18	64	F	Fibrosis + hepatitis [70]	2.87	273	111	36	813	1.0	3.49	(−)
19	45	F	Fibrosis + hepatitis [70]	1.46	125	33	18	20	1.0	4.11	(−)
20	53	M	Fibrosis + hepatitis [90]	0.7	140	150	80	242	1.0	4.68	(−)
21	44	F	Fibrosis + hepatitis [50]	0.44	184	29	20	875	1.0	3.97	(−)
22	41	M	Fibrosis + hepatitis [80]	1.35	121	35	40	147	1.0	4.26	(−)
23	50	M	Fibrosis + hepatitis [50]	1.45	121	44	29	86	1.0	4.7	(−)
24	39	M	Fibrosis + hepatitis [10]	6.42	2026	156	88	1338	1.0	n.e.	(−)
25	36	M	Fibrosis + hepatitis [30]	0.13	157	13	7	84	1.0	2.3	(−)
26	57	M	Cirrhosis/(C) [10]	2.42	416	43	35	242	1.3	3.25	(++)
27	48	F	Cirrhosis/(A) [90]	2.56	218	82	75	1185	1.1	4.78	(−)
28	66	M	Cirrhosis/(A) [10]	0.8	184	15	11	40	1.15	4.64	(−)
29	71	M	Cirrhosis/(B) [ne]	1.48	180	21	21	28	1.15	5.28	(+)
30	52	M	Cirrhosis/(A) [10]	0.81	168	18	10	186	1.15	4.52	(−)
31	44	M	Cirrhosis/(A) [60]	1.02	226	132	73	643	1.0	4.39	(−)
32	57	F	Cirrhosis/(B) [80]	1.2	428	34	17	957	1.2	2.98	(+).
33	41	M	Cirrhosis/(B) [50]	5.71	249	51	21	55	1.0	3.43	(−)
34	49	M	Cirrhosis/(A) [10]	0.36	258	24	20	55	1.05	n.e.	(−)
35	48	M	Cirrhosis/(B) [20]	1.27	177	68	46	92	1.0	3.84	(+)
36	42	M	Cirrhosis/(B) [50]	2.32	87	105	72	131	1.85	3.57	(++)
37	62	M	Cirrhosis/(B) [10]	1.69	175	14	5	195	1.3	3.94	(++)
38	74	F	Cirrhosis/(B/C) [50]	1.07	136	85	33	73	1.0	n.e.	(++)
39	52	M	Cirrhosis/(A) [70]	1.56	260	59	36	1546	1.3	4.72	(−)
40	43	M	Cirrhosis + hepatitis/(A) [10]	2.9	386	164	96	964	1.0	4.95	(−)

t-test using Microsoft® Excel and Origin® 6.1 (OriginLab, Northampton, MA, USA).

3. Results

In most examinations of this study, the PME and PDE resonance bands could be resolved into PE, PC, GPC, and GPE, respectively, with the exception of PME in six patients and in two healthy controls and PDE in three patients. Fig. 1b shows the fit of a ^{31}P MR spectrum of the liver of a healthy volunteer with well-resolved signals and only small PCr signal contamination from the abdominal wall.

Fig. 2a shows a representative {^{1}H}–^{31}P MR spectrum of a patient with alcoholic hepatic fibrosis, Fig. 2b a spectrum of a patient with alcoholic cirrhosis of the liver. The ratio PE/PC was found to be elevated in cirrhotics as compared to non-cirrhotics. Reduced ^{31}P signal-to-noise ratios were observed in patients with advanced ALD.

Fig. 3 shows a Box-and-Whiskers-Plot of the signal intensity ratio PME/PDE. The ratio PME/PDE was significantly elevated in C as compared to HC and NC ($P=0.002$ and $P=0.0002$, respectively), while NC and HC cannot be differentiated using this spectral parameter.

GPE/GPC in C and NC were significantly increased compared to HC ($P=0.002$ and $P=0.006$, respectively), with no significant difference in C compared to NC (Fig. 4).

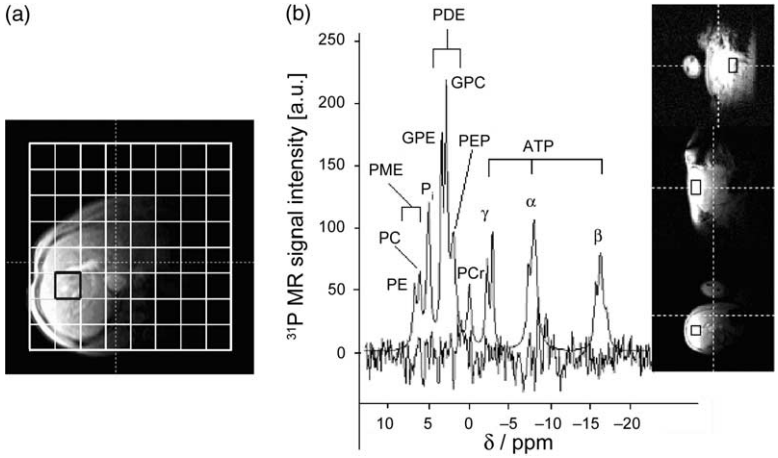

Fig. 1. {^{1}H}–^{31}P MRSI of the liver of a 22-year-old female healthy control. (a) Axial T_{1w} MR image of the liver obtained with a 14-cm-diameter surface coil; overlay: grid of ^{31}P MRSI (voxel size: 3.1×3.1×5.0 cm^3). (b) Fit of resonances and difference of in vivo {^{1}H}–^{31}P spectrum and fit. Resonances of PE, PC, P_i, GPE, GPC, PEP (phosphoenolpyruvate, according to [27]), residual PCr (from the muscle layer between coil and liver) and α-, β-, and γ-ATP are resolved. The low signal intensity of the PCr resonance indicates good spatial localisation of the voxel (rectangles) within the liver.

Signal intensity ratios of PE/PC were significantly elevated in C compared to HC and NC ($P=0.02$ and $P=0.05$, respectively) without significant difference of this parameter between HC and NC (Fig. 5).

No significant correlation of hepatic fat content (<30% vs. 30–60% vs. >60%) with PE/PC ratio (1.32±1.41 vs. 1.46±1.96 vs. 1.15±1.92, n.s. (not significant) and with GPE/GPC ratio (1.23±1.01 vs. 0.88±0.96 vs. 1.12±1.19, n.s. (not significant) was noted.

For all signal intensity ratios the data range was broader in C compared to HC.

4. Discussion

The data presented here show for the first time that {^{1}H} ^{31}P MRSI permits assessment of relative signal intensities of GPE, GPC, PE and PC in patients with ALD.

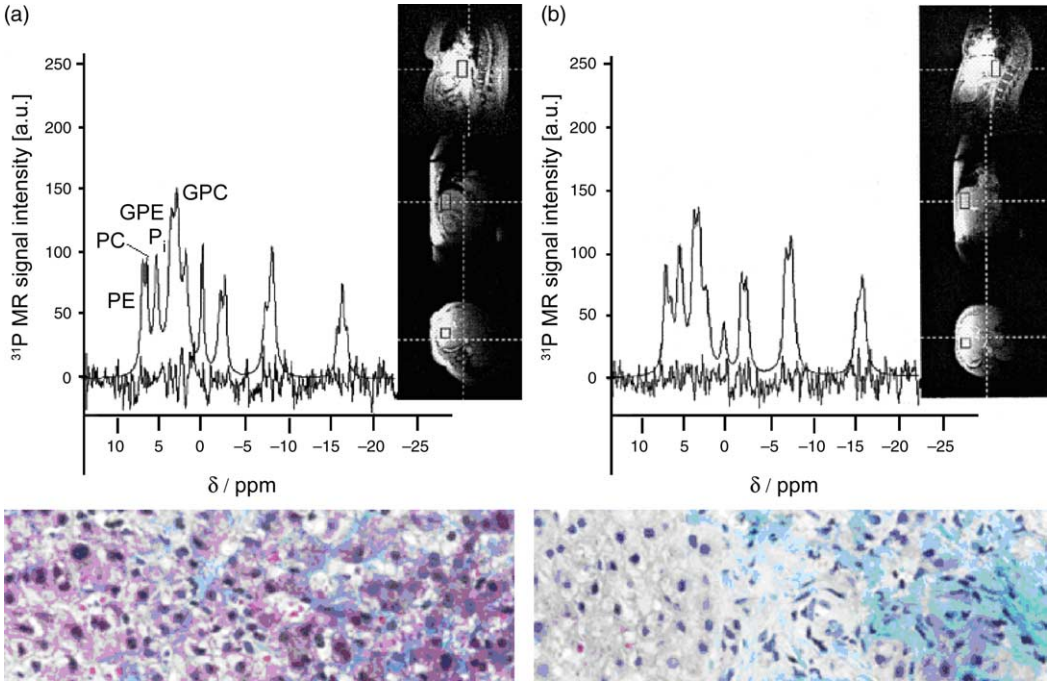

Fig. 2. (a) {^{1}H}–^{31}P MRSI spectrum and corresponding hepatic histology of a 55-year-old female patient with alcoholic liver fibrosis. The biopsy shows extensive periportal and parasinusoidal fibrosis in addition to typical ballooning of hepatocytes. (b) {^{1}H}–^{31}P MRSI spectrum and corresponding hepatic histology of a 49-year old male patient with cirrhosis of the liver. Biopsy shows micronodular alcoholic cirrhosis with typical pseudolobules. Compared to spectra of healthy controls (Fig. 1) and the patient with non-cirrhotic liver disease (Fig. 2a) increased PE/PC and compared to HC increased GPE/GPC ratios can be observed. The position of the observed voxel is indicated in orthogonal slices. [This figure appears in colour on the web.]

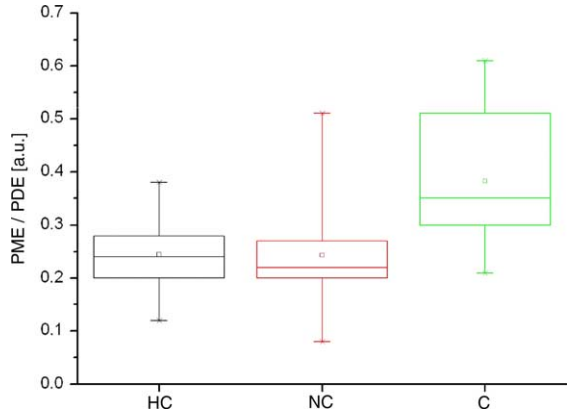

Fig. 3. Box-and-Whiskers-Plot of the signal intensity ratio of PME/PDE observed in healthy controls (HC), non-cirrhotics (NC) and cirrhotics (C). In C, PME/PDE is significantly elevated as compared to HC and NC ($P=0.002$/$P=0.0002$). No significant difference is observed between HC and NC. [This figure appears in colour on the web.]

With this technique it could be clearly demonstrated, that phospholipid metabolism is severely disturbed in ALD. ^{31}P MRSI has already been used in the past to study changes in high-energy phosphates, such as ATP, and changes in PME and PDE [24–26]. Proton decoupling enables further analysis of these phosphoesters. Proton decoupling enhances the spectral resolution and leads to a separation of the GPE and GPC, and PE and PC resonances, respectively. In addition, it achieves an approximately 30% enhancement of the signals by the nuclear Overhauser effect [28,29]. Therefore, this technique seems to be the method of choice to determine various PME and PDE in vivo. It is important to note, that no direct information from the lipid-soluble constituents of the membranes can be obtained. However, the MRS-detectable precursors (PE, PC) and degradation products (GPE, GPC) of phospholipids reflect the balance of anabolic and catabolic pathways.

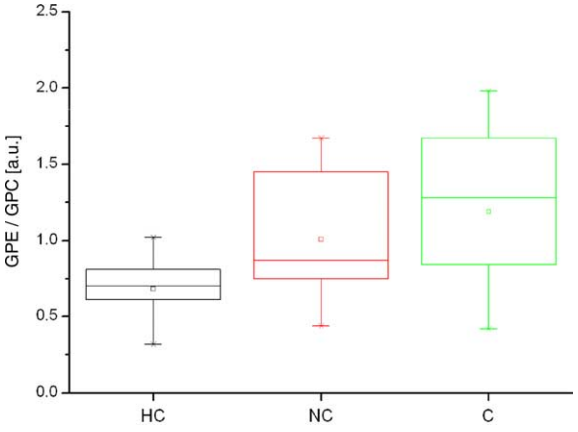

Fig. 4. Box-and-Whiskers-Plot of the signal intensity ratio of GPE/GPC observed in healthy controls (HC), non cirrhotics (NC) and cirrhotics (C). GPE/GPC is significantly elevated in C ($P=0.002$) and in NC ($P=0.006$) as compared to HC. No significant difference is observed between C and NC. [This figure appears in colour on the web.]

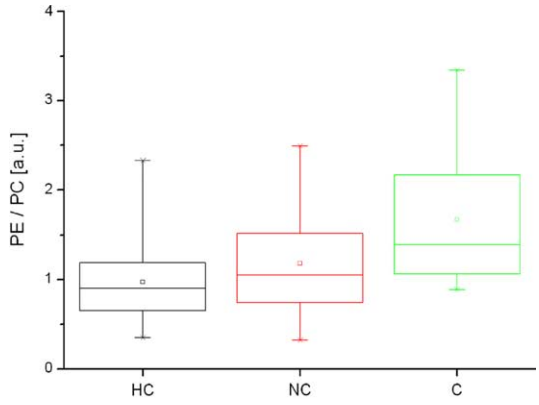

Fig. 5. Box-and-Whiskers-Plot of the signal intensity ratio of PE/PC observed in healthy controls (HC), non-cirrhotics (NC) and cirrhotics (C). In C, PE/PC is significantly elevated as compared to HC ($P=0.02$) and NC ($P=0.05$). No significant difference is observed between HC and NC. [This figure appears in colour on the web.]

The data reported here show an increase of the intensity ratios GPE/GPC in ALD and of PE/PC in cirrhotics, which mainly may result from either a decreased production of choline-containing compounds or an increased accumulation of ethanolamine-containing components or both within the hepatic membranes. These data confirm recent reports in the baboon which show a decrease in hepatic PPC after chronic alcohol consumption [3,6]. The pathogenesis of a relative decrease in hepatic GPC and PC and/or a relative increase in hepatic GPE and PE following chronic alcohol consumption and in ALD may involve various mechanisms.

Besides the fact that the availability of methyl groups and also the activation of methionine to SAM following alcohol ingestion is limited [7,9–13], an important observation seems to be the inhibition of PEMT by acetaldehyde [7,8]. PEMT is an enzyme that catalyses the stepwise methylation of phosphatidylethanolamine to phosphatidylcholine. Phosphatidylcholine can be synthesized by two pathways. The major route for phosphatidylcholine synthesis in most cells is via the cytidinediphosphocholine pathway. However, in the liver an alternative pathway, namely phosphatidylethanolamine-*N*-methylation, is responsible for approximately 30% of phosphatidylcholine synthesis and this process can be stimulated when methionine is provided [32]. Besides the fact that an inhibition of PEMT by acetaldehyde leads to a decreased synthesis of GPC and therefore to morphologic and functional changes in biomembranes, PEMT also contributes to the control of hepatocyte cell division since its inactivation is associated with several types of hepatic proliferation [33] including carcinogenesis [34,35]. It is noteworthy that PEMT is permanently inactivated in liver cancer induced by the Solt and Faber model [36], and it has been shown that the loss of PEMT activity may contribute to malignant transformation of hepatocytes [36]. Thus, if indeed the changes in phospholipid metabolism observed in our study are

primarily the consequence of an alcohol-mediated inhibition of PEMT, this effect could play a role in alcohol-associated hepatocarcinogenesis. It has been demonstrated that chronic alcohol consumption is a risk factor for hepatocellular cancer [37], and this is especially relevant in alcoholics who produce more acetaldehyde following ethanol consumption due to a polymorphism in the alcoholdehydrogenase 1C gene [38].

It is interesting to note that the GPE/GPC ratios as measured non-invasively by in vivo $\{^1H\}$–^{31}P MRSI can distinguish early-stage ALD from HC, but not cirrhotic ALD from non-cirrhotic ALD. This may be explained by the fact that ethanol itself, regardless of the severity of ALD, leads to a change in the ratio of the biomembrane precursors, namely PE and PC, which will not increase further during progression of the disease. On the other hand, the ratio PE/PC allows to distinguish advanced from early ALD similar to the PME/PDE ratio. It cannot be excluded that the levels of the biomembrane precursors PE and PC are not only affected by ethanol-mediated metabolic alterations, but also by metabolic mechanisms generally observed in advanced liver disease such as limited availability of methionine.

Although choline deficiency may promote hepatic steatosis, we could not detect any relationship between hepatic fat content, determined histologically, and PE/PC or GPE/GPC ratios, possibly due to the limited number of observations. In any case, one important result of this study is that ratios of GPE/GPC and of PE/PC determined non-invasively by $\{^1H\}$–^{31}P MRSI may be used as an index which is capable to distinguish between C and NC in ALD patients.

Besides the fact that composition of the various PME and PDE in the liver was significantly altered in ALD, ^{31}P MRSI identified other changes of hepatic phospholipids. Patients with cirrhosis of the liver had a significant decrease of the total phosphorous MRS signal, which may reflect reduction of the functioning liver cell mass [22]. In particular, the level of ATP was reduced, indicating a decrease of the hepatic energy state which is in agreement with earlier ^{31}P MRS observations of Meyerhoff et al. [15]. In this context, it is interesting to note that also in non-alcoholic fatty liver disease ATP levels were found to be reduced [39]. Finally, PME/PDE ratios were significantly increased in cirrhotics but not in non-cirrhotics as compared to controls. This observation, however, is not new and was already discussed several years ago. Menon et al. reported an elevation of PME/ATP and PDE/ATP ratios in alcoholics without significant liver injury [26]. This finding was interpreted as a change in hepatic redox state due to ethanol metabolism and as an induction of the hepatocyte endoplasmic reticulum. In alcoholic hepatitis PME concentrations were found to be increased and could even be correlated with the severity of the disease [24].

Similar results have been reported for alcoholic cirrhosis [16,20], but could not be confirmed by other groups [15,25]. Most recently, an increase in PME/PDE ratios in chronic hepatitis C from moderate disease to cirrhosis has been observed using conventional ^{31}P MRS [21], and these new observations confirm earlier results in viral hepatitis [15]. This contradicts the data of van Wassenaer-van Hall et al. who could not differentiate fibrosis from cirrhosis in patients with various etiologies of liver disease [23]. The authors concluded that ^{31}P MRS is a poor tool for classifying patients into diagnostical categories of liver injury. The controversial results of these different publications can possibly be attributed to the heterogeneity of the etiologies of liver disease studied. The use of $\{^1H\}$–^{31}P MRSI as in the present study provided an additional advantage to distinguish moderate from severe liver disease, at least due to chronic alcohol ingestion. However, it is not clear whether the observed alterations in hepatic phospholipid metabolism are specific for chronic alcohol consumption or whether similar alterations in phospholipid metabolism may also be present in cirrhotic livers of other etiologies. The data of a disturbed phospholipid metabolism following chronic alcohol consumption in man are of particular interest in the light of the fact, that in the baboon ALD could be prevented when those animals were fed PPC-enriched diets [5,40].

Most recently, results of a large randomised control multicenter trial from the US were presented, in which the impressive number of 789 patients with biopsy-proven ALD were treated with 1.5 g of PPC per day or placebo for 4–6 years [41]. By the overall comparison of the two groups the data showed a significant treatment effect with PPC, which, however, can also be attributed to their marked reduction of alcohol consumption. A subgroup of 52 patients who continued to drink at least 6 drinks per day, showed a slight regression with PPC, whereas those on placebo progressed histologically. It would be of interest to know, whether the patients who showed a beneficial effect of PPC-treatment also had alterations in hepatic phospholipid metabolism. $\{^1H\}$–^{31}P MRSI could be an appropriate tool not only to detect those patients with an altered phospholipid metabolism due to alcohol as candidates for PPC treatment, but also to monitor these patients during treatment. Moreover, correlations can be looked for between changes of PE/PC and GPE/GPC ratios and histological improvement following treatment with PPC. The technique may allow to prove whether the alteration of hepatic phospholipid metabolism indeed plays a major role in the pathogenesis of ALD. Therefore, further clinical studies should correlate $\{^1H\}$–^{31}P MRSI with biochemical analysis of actual PE and PC concentrations in liver tissue. Subsequently, attempts should be made to evaluate the sensitivity and specifity of the technique for its clinical application.

References

[1] Yamada S, Mak M, Lieber CS. Chronic ethanol consumption alters rat liver plasma membranes and potentiates release of alkaline phosphatase. Gastroenterology 1985;88:1799–1806.

[2] Lieber CS, Leo MA. Alcohol and the liver. In: Lieber CS, editor. Medical and nutritional complications of alcoholism: mechanisms and management. New York: Plenum Press; 1992. p. 185–240.
[3] Arai M, Leo MA, Nakano M, Lieber CS. Biochemical and morphological alterations of baboon hepatic mitochondria after chronic ethanol consumption. Hepatology 1984;4:165–174.
[4] Arai M, Gordon ER, Lieber CS. Decreased cytochrome oxidase activity in hepatic mitochondria after chronic alcohol consumption and possible role of decreased cytochrome a3 content and changes in phospholipids. Biochem Biophys Acta 1984;797:320–327.
[5] Lieber CS, DeCarli LM, Mak KM, Kim CI, Leo MA. Attenuation of alcohol-induced hepatic fibrosis by polyunsaturated lecithin. Hepatology 1990;12:1390–1398.
[6] Lieber CS. Alcoholic liver disease: new insights in pathogenesis lead to new treatments. J Hepatol 2000;32:113–128.
[7] Duce AM, Ortiz P, Cabrero C, Mato JM. *S*-Adenosyl-L-methionine synthetase and phospholipid methyltransferase are inhibited in human cirrhosis. Hepatology 1988;8:65–68.
[8] Lieber CS, Robins SJ, Leo MA. Hepatic phosphatidylethanolamine methyltransferase activity is decreased by ethanol and increased by phosphatidylcholine. Alcohol Clin Exp Res 1994;18(3):592–595.
[9] Stickel F, Seitz HK. Ethanol- and methyl transfer: its role in liver disease and hepatocarcinogenesis. In: Watson RR, Preedy VR, editors. Nutrition and alcohol: linking nutrient interactions and dietary intake. Washington, DC: CRC Press; 2004.
[10] Stickel F, Choi SW, Kim YI, Bagley PJ, Seitz HK, Russel RM, et al. Effect of chronic alcohol consumption on total plasma homocystein level in rats. Alcohol Clin Exp Res 2000;24:259–264.
[11] Shaw S, Jayatilleke E, Herbert V, Colman N. Cleavage of folates during ethanol metabolism: role of acetaldehyde/xanthine oxidase generated superoxide. Biochem J 1989;257:277–281.
[12] Halsted CH, Villanueva J, Chandler CJ, Stabler SP, Allen RH, Muskhelishivili L, et al. Ethanol feeding of micropigs alters methionine metabolism and increases hepatocellular apoptosis and proliferation. Hepatology 1996;23:497–505.
[13] Avila MA, Garcia-Trevijano ER, Martinez-Chantar ML, Latasa MU, Perez-Mato I, Martinez-Cruz LA, et al. *S*-Adenosylmethionine revisited: its essential role in the regulation of liver function. Alcohol 2002;27:163–167.
[14] Cox IJ, Bryant DJ, Collins AG, George P, Harman RR, Hall AS, et al. Four-dimensional chemical shift MR imaging of phosphorous metabolites of normal and diseased human liver. J Comput Assist Tomogr 1988;12:369–376.
[15] Meyerhoff DJ, Boska MD, Thomas AM, Weiner MW. Alcoholic liver disease: quantitative image guided P-31 MR spectroscopy. Radiology 1989;173:393–400.
[16] Oberhaensli R, Rajagopalan B, Galloway GJ, Taylor DJ, Radda GK. Study of human liver disease with P-31 magnetic resonance spectroscopy. Gut 1990;31:463–467.
[17] Cox IJ, Menon DK, Sargentoni J, Bryant DJ, Collins AG, Coutts GA, et al. Phosphorus-31 magnetic resonance spectroscopy of the human liver using chemical shift imaging techniques. J Hepatol 1992;14: 265–275.
[18] Taylor-Robinson SD, Sargentoni J, Bell JD, Saeed N, Changani KK, Davidson BR, et al. In vivo and in vitro hepatic ^{31}P magnetic resonance spectroscopy and electron microscopy of the cirrhotic liver. Liver 1997;17:198–209.
[19] Jalan R, Sargentoni J, Coutts GA, Bell JD, Rolles K, Burroughs AK, et al. Hepatic phosphorus-31 magnetic resonance spectroscopy in primary biliary cirrhosis and its relation to prognostic models. Gut 1996;39:141–146.
[20] Munataka T, Griffiths RD, Martin PA, Jenkins SA, Shields R, Edwards RHT. An in vivo ^{31}P MRS study of patients with liver cirrhosis: progress toward a non-invasive assessment of disease severity. NMR Biomed 1993;6:168–172.
[21] Lim AKP, Patel N, Hamilton G, Hajnal JV, Goldin RG, Taylor-Robinson SD. The relationship of in vivo ^{31}P MR spectroscopy to histology in chronic hepatitis C. Hepatology 2003;37(4): 788–794.
[22] Menon DK, Sargentoni J, Taylor-Robinson SD, Bell JD, Cox IJ, Bryant DJ, et al. Effect of functional grade and etiology on in vivo hepatic phosphorus-31 magnetic resonance spectroscopy in cirrhosis: biochemical basis of spectral appearances. Hepatology 1995;21: 417–427.
[23] Van Wassenaer-van Hall HN, van der Grond J, van Hattum J, Kooijman C, Hoogenraad TU, Mali WPTM. ^{31}P magnetic resonance spectroscopy of the liver: correlation with standardized serum, clinical and histological diagnosis in diffuse liver disease. Hepatology 1995; 21:443–449.
[24] Angus PW, Dixon RM, Rajagopalan B, Ryley NG, Simpson KJ, Peters TJ, et al. A study of patients with alcoholic liver disease by ^{31}P nuclear magnetic resonance spectroscopy. Clin Sci 1990;78: 33–38.
[25] Rajanayagam V, Lee RR, Ackerman Z, Bradley WG, Ross BD. Quantitative P-31 MR spectroscopy of the liver in alcoholic cirrhosis. J Magn Reson Imaging 1992;2:183–190.
[26] Menon DK, Harris M, Sargentoni J, Taylor-Robinson SD, Cox IJ, Morgan MY. In vivo hepatic ^{31}P magnetic resonance spectroscopy in chronic alcohol abusers. Gastroenterology 1995;108:776–788.
[27] Luyten PR, Bruntink G, Sloff FM, Vermeulen JWAH, van der Heijden JL, den Hollander JA, et al. Broadband proton decoupling in human ^{31}P NMR spectroscopy. NMR Biomed 1989;1:177–183.
[28] Bachert P, Ermark F, Zabel H-J, Sauter R, Semmler W, Lorenz WJ. In vivo nuclear Overhauser effect in ^{31}P–{^{1}H} double resonance experiments in a 1.5 T whole-body MR system. Magn Reson Med 1990;15:165–172.
[29] Bachert P, Bellemann ME. Kinetics of the in vivo ^{31}P–^{1}H nuclear Overhauser effect of the human-calf-muscle phosphocreatine resonance. J Magn Reson 1992;100:146–156.
[30] Li CW, Negendank WG, Murphy-Boesch J, Padavic-Shaller K, Brown TR. Molar quantitation of hepatic metabolites in vivo in proton decoupled nuclear Overhauser effect enhanced ^{31}P NMR spectra localized by three dimensional chemical shift imaging. NMR Biomed 1996;9:141–155.
[31] Bachert P, Bellemann ME, Layer G, Koch T, Semmler W, Lorenz WJ. In vivo ^{1}H, ^{31}P–{^{1}H} and ^{13}C–{^{1}H} magnetic resonance spectroscopy of malignant histiocytoma and skeletal muscle tissue in man. NMR Biomed 1992;5:161–170.
[32] Sundler R, Akesson B. Regulation of phospholipid biosynthesis in isolated rat hepatocytes. J Biol Chem 1975;250:3359–3367.
[33] Tessitore L, Cui Z, Vance DE. Transient inactivation of phosphatidylethanolamine-*N*-methyltransferase-2 and activation of cytidine triphosphate: phosphocholine cytidylyl-transferase during nonneoplastic growth. Biochem J 1997;322:151–154.
[34] Cui Z, Houweling M, Vance DE. Suppresssion of rat hepatoma cell growth by expression of phosphatidylethanolamine *N*-methyltransferase-2. J Biol Chem 1994;269:24531–24538.
[35] Tessitore L, Sesca E, Bosco M, Vance DE. Expression of phosphatidylethanolamine-*N*-methyltransferase in Yoshida ascites hepatoma cells and the livers of host rats. Carcinogenesis 1999;20: 561–567.
[36] Tessitore L, Sesca E, Vance DE. Inactivation of phosphatidylethanolamine-*N*-methyltransferase-2 in aflatoxin-induced liver cancer and partial reversion of the neoplastic phenotype by PEMT transfaction of hepatoma cells. Int J Cancer 2000;86:362–367.
[37] Stickel F, Schuppan D, Hahn EG, Seitz HK. Cocarcinogenic effects of alcohol in hepatocarcinogenesis. Gut 2002;51:132–139.
[38] Stickel F, Homan N, Benesova M, Jacubs A, Schuppan D, Hahn EG, et al. Genetic predisposition for alcohol associated upper aerodigestive tract cancer and hepatocellular carcinoma in heavy drinkers with the alcoholdehydrogenase 3*1 allel. Gastroenterology (abstract) 2003;124:A547.

[39] Cortez-Pinto H, Catham J, Chacko VP, Arnold C, Rashid A, Diehl AM. Alterations in liver ATP homeostasis in human non-alcoholic steatohepatitis: a pilot study. J Am Med Assoc 1999;282:1659–1664.
[40] Lieber CS, Robins SJ, Li JJ, DeCarli LM, Mak KM, Fasulo JM, et al. Phosphatidylcholine protects against fibrosis and cirrhosis in the baboon. Hepatology 1994;12:1390–1398.
[41] Lieber CS, Weiss DG, Point P, Groszmann R, Paronetto F, Schenker S, et al. Effect of moderation of ethanol consumption combined with PPC administration on liver injury in alcoholics: prospective, randomized, placebo controlled, multicenter VA trial (CSP 391). Hepatology (abstract) 2002;36: 381A.